Contribution from the Departments of Chemistry, University of Notre Dame, Notre Dame, Indiana 56556, and University of Wisconsin, Madison, Wisconsin 53706

Application of the Fenske–Hall Molecular Orbital Method to the Calculation of ^{11}B NMR Chemical Shifts. Antipodal Substituent Effects in Deltahedral Clusters

Thomas P. Fehlner,*,† Paul T. Czech,‡ and Richard F. Fenske*,‡

Received December 7, 1989

Utilizing Fenske–Hall wave functions and eigenvalues combined with the Ramsey sum over states (SOS) approximation, we demonstrate that the sign and magnitude of the "paramagnetic" contribution to the shielding correlates well with the observed ^{11}B chemical shifts of a substantial variety of boron- and metal-containing compounds. Analysis of the molecular orbital (MO) contributions in the SOS approximation leads to an explanation of the large downfield shifts associated with metal-rich metallaboranes. A similar analysis demonstrates the importance of selected cluster occupied and unoccupied MO's in explaining both exo-cage substituent effects in which the antipodal boron resonance is shifted upfield and endo-cage substituent effects (interchange of isolobal fragments within the cage framework) in which the antipodal boron resonance is shifted downfield. Exo- and endo-cage substitution perturbs these MO's in an understandable fashion, leading to an internally consistent explanation of the observed chemical shift changes.

The response of materials to a perturbation induced by a magnetic field constitutes a classical and valuable source of information on electronic structure.[1] The advent of nuclear magnetic resonance spectroscopy as the structural tool of choice of the experimental chemist for many problems has resulted in the creation of a large body of data consisting in the relative shielding of NMR active nuclei in a variety of chemical environments.[2-4] These data constitute an extremely valuable source of information on the structural environment of a given nucleus. Despite many efforts, attempts to connect chemical shifts of nuclei in large molecules to quantum chemical models of electronic structure have generated essentially empirical parametrized fits.[5] In such correlations the connection between electronic structure and chemical shift is a tenuous one. To fully exploit the information on electronic structure contained in the chemical shifts of nuclei in molecules, a usable, unambiguous method of connecting relative shieldings to the molecular orbital (MO) properties of a chemical species is required.

The Fenske–Hall method is a proven MO method that is often chosen to characterize the electronic structure of complex systems presently beyond the limits of more exact methods.[6] Recent work has now demonstrated that the Fenske–Hall wave functions and energies provide an approximate, but workable, approach to the calculation of the ^{13}C chemical shifts of a variety of organometallic compounds.[7] As several groups have noted a simple relationship between ^{13}C and ^{11}B NMR chemical shifts for related compounds,[8] we have been led to the application of Fenske–Hall wave functions to an investigation of the shielding of ^{11}B nuclei. Our first objective was to investigate the applicability of this approach to a nucleus other than carbon. If successful, we wished to explore the electronic origins of well-known, but poorly understood, phenomena in the ^{11}B spectra of cluster compounds. The two considered below are the extreme low-field chemical shifts observed for metal-rich metallaboranes and the impressive cross-cage (antipodal) substituent effects reported in the ^{11}B spectra of borane and heteroborane cages.

General Correlation. The normal range of ^{11}B chemical shifts lies between δ +80 and −50 ppm (δ = 0 for $BF_3{\cdot}Et_2O$) with the negative values corresponding to a shielding of the sample larger than that of $BF_3{\cdot}Et_2O$.[9] Recently, a significant number of "metal-rich" metallaboranes have been characterized[10] that exhibit large positive chemical shifts (shielding less than that of $BF_3{\cdot}Et_2O$), e.g., δ = 211 for $[Rh_2Fe_4(CO)_{16}B]^-$,[11] which allowed an empirical parameterization for a set of related ferraboranes.[12] In doing so it was determined for the ferraboranes that increasing positive chemical shift was accompanied by an increasing Mulliken population on the boron atom. Earlier investigators, however, indicated that for a substantial set of metal-free boranes, an increasing positive chemical shift was accompanied by a *decreasing* Mulliken population on the boron atom.[13] Clearly the correlation of chemical shift with boron populations proved unreliable, and these kinds of correlations between chemical shifts and MO parameters, even if of some empirical value, provide little understanding of the electronic origins of ^{11}B shifts. Rather than seeking correlations of chemical shift with parameters processed from the MO's, an alternative approach is to go back to the wave functions themselves.

Ramsey[14] treated the problem of a molecule in a magnetic field by expressing the total wave function in terms of the set of wave functions of the unperturbed molecule. This led to the now familiar two-term expression for the shielding tensor given in (1).[15]

$$\sigma = \sigma_d + \sigma_p \qquad (1)$$

The first term, the so-called diamagnetic term, depends only on the ground-state wave function while the second term, the paramagnetic term, depends on the ground- and excited-state wave functions. These terms act in opposite directions, and the paramagnetic term is different from zero only for electrons with orbital angular momentum. Hence, the relatively small chemical shift range observed for the ^1H nucleus is often attributed to the fact that σ_p is essentially zero in the Ramsey expression for the total shielding. It follows that the much larger chemical shift ranges exhibited by nuclei other than ^1H can attributed to large changes

† University of Notre Dame.
‡ University of Wisconsin.

(1) Eyring, H.; Walter, J.; Kimball, G. E. *Quantum Chemistry*; Wiley: New York, 1944.
(2) Pople, J. A.; Schneider, W. G.; Bernstein, H. J. *High Resolution NMR*; McGraw-Hill: New York, 1959.
(3) Harris, R. K.; Mann, B. E., Eds. *NMR and the Periodic Table*; Heyden: London, 1978.
(4) Laszlo, P., Ed. *NMR of Newly Accessible Nucle*; Academic: New York, 1983; Vols. 1 and 2.
(5) Hafner, A.; Hegedus, L. S.; de Weck, G.; Hawkins, B.; Dotz, K. H. *J. Am. Chem. Soc.* **1988**, *110*, 8413. For ^{11}B NMR, see, for example: Teixidor, F.; Vinas, C.; Rudolph, R. W. *Inorg. Chem.* **1986**, *25*, 3339. Hermânek, S., Ed. *Boron Chemistry*; World Scientific: Teaneck, NJ, 1987; p 26.
(6) Hall, M. B.; Fenske, R. F. *Inorg. Chem.* **1972**, *11*, 768. Hall, M. B. Ph.D. Thesis, University of Wisconsin, Madison, WI, 1971. Fenske, R. F. *Pure Appl. Chem.* **1971**, *27*, 61.
(7) Czech, P. T.; Ye, X. Q.; Fenske, R. F. *Organometallics*, in press.
(8) Williams, R. E.; Field, L. D. In *Boron Chemistry-4*; Parry, R. W., Kodama, G., Eds.; Pergamon: New York, 1980. Spielvogel, B. F.; Nutt, W. R.; Izydore, R. A. *J. Am. Chem. Soc.* **1975**, *97*, 1609. Spielvogel, B. F.; Purser, J. M. *J. Am. Chem. Soc.* **1971**, *93*, 4418. Nöth, H.; Wrackmeyer, B. *Chem. Ber.* **1974**, *107*, 3089.
(9) Kidd, R. G. In *NMR of Newly Accessible Nuclei*; Laszlo, P., Ed.; Academic: New York, 1983; Vol. 2, p 50.
(10) Fehlner, T. P. *New J. Chem.* **1988**, *12*, 307.
(11) Khattar, R.; Puga, J.; Fehlner, T. P.; Rheingold, A. L. *J. Am. Chem. Soc.* **1989**, *111*, 1877.
(12) Rath, N. P.; Fehlner, T. P. *J. Am. Chem. Soc.* **1988**, *110*, 5345.
(13) Kroner, J.; Wrackmeyer, B. *J. Chem. Soc., Faraday Trans. 2* **1976**, *72*, 2283. Note that the pre-1976 sign convention for the ^{11}B chemical shift is used in this paper.
(14) Ramsey, N. F. *Phys. Rev.* **1950**, *78*, 699.
(15) Ando, I.; Webb, G. A. *Theory of NMR Parameters*; Academic: New York, 1983.

0020-1669/90/1329-3103$02.50/0

Scheme I

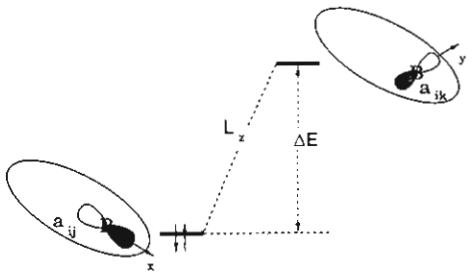

in the paramagnetic term.[16] On the other hand, as σ_d and σ_p can be of similar magnitude but of opposite sign, neither, in principle, should be neglected in a calculational approach. Despite this, we have previously demonstrated that the Fenske–Hall MO's and associated energies yield values of the paramagnetic component of the shielding that correlate well with observed ^{13}C chemical shifts. This implies that the diamagnetic term can be treated as if constant and need not be explicitly calculated. We take the same approach below for the ^{11}B nucleus.

Introducing the LCAO-SCF approximation yields the expression for the paramagnetic term given in eq 2, where the indices

$$\sigma_p^n(B) = -\mu_0 e^2/8\pi m^2 \sum\sum (E_k - E_j)^{-1}[\langle \Phi_j|L_n|\Phi_k\rangle \times \langle \Phi_k|L_{B_n} r_B^{-3}|\Phi_j\rangle + \langle \Phi_j|L_{B_n} r_B^{-3}|\Phi_k\rangle\langle \Phi_k|L_n|\Phi_j\rangle] \quad (2)$$

j and k span the filled and unfilled MO's, respectively, and n spans x, y, and z. This constitutes the sum-over-states (SOS) expression for the paramagnetic component of the overall shielding and includes the virtual MO's as a representation of the excited state wave functions of the unperturbed molecule. This is at best a crude approximation and for the high-lying excited states is grossly inappropriate. It is only usable because of the $(E_k - E_j)^{-1}$ term, which only allows significant contributions to expression 2 to arise from terms involving high-lying filled and low-lying unfilled MO's. Moreover, the expression in eq 2 shows that σ_p is significantly different from zero only when three criteria are simultaneously satisfied. First, since it appears in the denominator, $E_k - E_j$, the energy difference between the virtual orbital, Φ_k, and the occupied orbital, Φ_j, must be small. Second, because of the $1/r_B^3$ dependence of the L/r^3 operator, the contributions of the atomic functions on the specified boron atom to both the filled and virtual orbitals must be significant. Third, the boron orbitals involved must be of proper symmetry to be coupled by the L operator. The last condition can be appreciated by noting that for the L_z operator on an isolated boron atom only the terms $\langle B_{2p_y}|L_z|B_{2p_x}\rangle$ and $\langle B_{2p_x}|L_z|B_{2p_y}\rangle$ are nonzero. However, it is important to note that contributions to the molecular matrix element, $\langle \Phi_k|L_n|\Phi_j\rangle$, can arise from terms on atomic centers other than the boron atom of interest, such as $\langle B_{2p_x}(2)|L_z(1)|B_{2p_y}(2)\rangle$ where $L_z(1)$ refers to the operator placed on boron center 1 while the two boron functions are on boron center 2. Such interactions are particularly important in systems where the contributions by centers 1 and 2 are equal by the symmetry of the molecule. Specific examples of such interactions will be cited in a later section.

As summarized in Scheme I in which the term $[1/(E_k - E_j)]\langle B_{2p_y}|L_z|B_{2p_z}\rangle$ is represented schematically, only high-lying filled and low-lying unfilled MO's with large B_{2p} AO components having the proper symmetry will contribute to the paramagnetic term. Hence, a significant fraction of the terms in the double sum in eq 2 are negligible, and for molecules with high symmetry, a simple picture of the origin of σ_p is feasible. Note that similar considerations apply to the $\langle \Phi_k|L_{B_n} r_B^{-3}|\Phi_j\rangle$ term as well.

Standard Fenske–Hall calculations utilizing only geometric structure and AO wave functions as input have been carried out on the molecules in Table I. MO's and their associated energies were then used to explicitly calculate the L_x, L_y, and L_z components of σ_p from eq 2. The reported values of the ^{11}B chemical shifts,

(16) Reference 15, p 50.

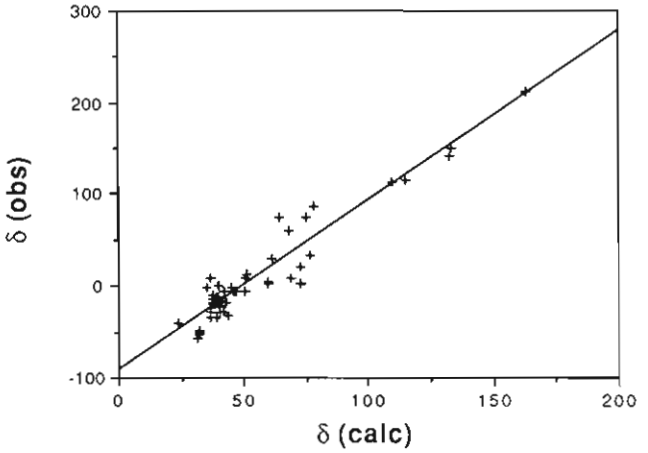

Figure 1. General correlation of δ(obs) and δ(calc) for the boron-containing compounds given in Table I. The equation of the straight line is $y = -91.9731 + 1.8452x$; $R = 0.95$.

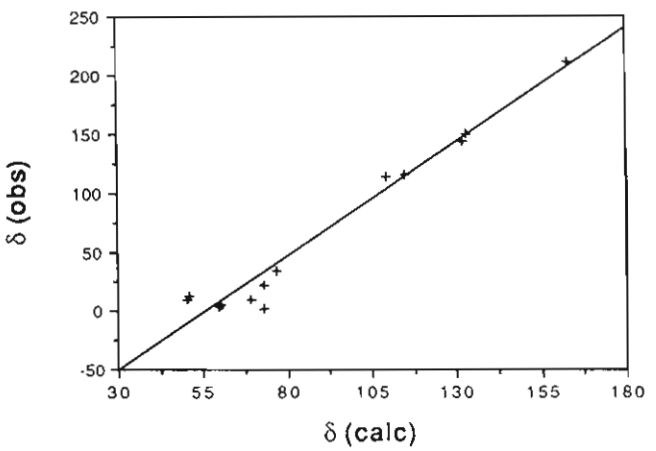

Figure 2. Correlation of δ(obs) and δ(calc) for all metallaboranes in Table I. The equation of the straight line is $y = -110.6414 + 1.9443x$; $R = 0.98$.

δ(obs), and the calculated paramagnetic contributions to the ^{11}B shift, σ_p, for a wide variety and representative sample of compounds containing a total of 64 boron atoms are given in Table I. As $\delta = \sigma(\text{reference}) - \sigma(\text{sample})$, it follows from using eq 1 that $\delta(\text{calc}) = [\sigma_d(\text{ref}) - \sigma_d(\text{sample})] + [\sigma_p(\text{ref}) - \sigma_p(\text{sample})]$. The first bracketed term is assumed to be constant (see above), and $\sigma_p(\text{ref})$ is chosen to be zero for convenience, i.e., $\delta(\text{calc}) = -\sigma_p(\text{sample}) + \text{constant}$. In Figure 1, δ(obs) and δ(calc) are compared and the correlation is good considering the fact that σ_d has been ignored.

Several observations can be made concerning the results displayed in Figure 1. First of all, the scatter in the correlation shows that this approach is not sufficiently precise to allow structural conclusions to be drawn from a calculated σ_p for any compound of unknown structure. Secondly, one notes that the slope of the correlation is significantly greater than 1. This can be ascribed to the fact that the Fenske–Hall MO's (filled and unfilled) have a much higher spread of energies than those of more exact methods due to the fact that electron–electron repulsions are not adequately treated. Because of the ΔE term in (2), this will lead to low values of the shielding factor and slopes greater than 1.

One might expect to minimize the fluctuations of such a systematic error if only related compounds are compared. Indeed, such is the case for the metallaboranes and the 10-atom closo cages where more precise correlations are shown in Figures 2 and 3 between δ(obs) and δ(calc), albeit with different slopes. Note that these results are equal or better than previously published empirical correlations for similarly restricted sets of compounds. Clearly valid qualitative conclusions concerning the chemical environment of a boron atom result from the calculations. For example, for the metal-rich metallaboranes, the large negative σ_p clearly indicate

Table I. Observed ^{11}B Chemical Shifts and Calculated "Paramagnetic" Contributions to the Chemical Shift

molecule	position	δ(obs)	σ_p(calc)	ref	molecule	position	δ(obs)	σ_p(calc)	ref
$[BH_4]^-$		−41.2	−23.92	*b*	2-I-1,6-$C_2B_4H_5$	2	−32.7	−43.42	*i*
BMe_3		86.0	−77.94	*b*		3, 5	−15.9	−40.74	
B_5H_9	1	−53.1	−32.47	*b*		4	−20.1	−38.47	
	2	−13.4	−38.59		2-Me-1,6-$C_2B_4H_5$	2	−5.9	−41.95	*j*
2-FB_5H_8	1	−56.6	−31.40	*c*		3, 5	−15.1	−40.44	
	2	8.0	−36.65			4	−19.3	−39.68	
	3, 5	−18.3	−37.92		$[B_{10}H_{10}]^{2-}$	1, 10	−4.7	−50.43	*k*
	4	−34.3	−36.58			2–9	−34.7	−38.89	
2-ClB_5H_8	1	−52.2	−31.82	*d*	1-SB_9H_9	2–5	−4.8	−46.07	*l*
	2	−1.1	−35.12			6–9	−17.6	−42.53	
	3, 5	−13.7	−38.22			10	74.5	−64.61	
	4	−23.4	−36.67		1-NB_9H_{10}	2–5	−6.1	−46.55	*m*
2-BrB_5H_8	1	−52.5	−31.97	*d*		6–9	−21.5	−40.81	
	2	−10.9	−39.71			10	61	−67.85	
	3, 5	−13.9	−38.40		$[(1\text{-}CpNi)B_9H_9]^-$	2–5	29.0	−61.47	*n*
	4	−19.9	−37.29			6–9	−1.3	−45.08	
2-IB_5H_8	1	−47.8	−32.36	*e*		10	73.6	−74.99	
	2	−28.0	−40.89		$B_3H_7Fe_2(CO)_6$	1, 3	4.2	−60.08	*o*
	3, 5	−11.4	−38.72			2	12.4	−51.09	
	4	−14.4	−37.66		$[B_3H_6Fe_2(CO)_6]^-$	1	33.7	−76.85	*p*
2-MeB_5H_8	1	−51.6	−32.36	*c*		2	8.6	−50.55	
	2	1.4	−39.84			3	2.4	−59.70	
	3, 5	−13.9	−38.65		$HFe_3(CO)_9BH_4$		2	−73.08	*q*
	4	−19.3	−38.16		$HFe_3(CO)_9BH_3Me$		22	−73.01	*q*
1,6-$C_2B_4H_6$	2–5	−18.7	−40.35	*f*	$HFe_4(CO)_{12}BH_2$		116	−114.66	*r*
2-F-1,6-$C_2B_4H_5$	2		−38.93		$[HFe_4(CO)_{12}BH]^-$		150	−133.14	*r*
	3, 5		−40.17		$[Rh_2Fe_4(CO)_{16}B]^-$		211	−163.18	*s*
	4		−36.83		$Cp_3Co_3BPhPPh$		143	−132.19[a]	*t*
2-Cl-1,6-$C_2B_4H_5$	2	−8.8	−37.79	*g*	$Cp_4Co_4B_2H_4$		114	−109.34	*u*
	3, 5	−16.4	−40.43		$HFe_4(CO)_{12}CBH_2$		9	−69.00	*v*
	4	−28.0	−36.76						
2-Br-1,6-$C_2B_4H_5$	2	−27.7	−42.31	*h*					
	3, 5	−16.3	−40.24						
	4	−18.2	−37.89						

[a] Calculated for Cp_3Co_3BHPH. Note that the observed shift for Cp_3Co_3BHPPh is 141. [b] Eaton, GR.; Lipscomb, W. N. *NMR Studies of Boron Hydrides and Related Compounds*; Benjamin: New York, 1969. [c] Burg, A. B. *J. Am. Chem. Soc.* **1968**, *90*, 1407. [d] Gaines, D. F.; Martens, J. A. *Inorg. Chem.* **1968**, *7*, 704. [e] Burg, A. B.; Sandhu, J. S. *J. Am. Chem. Soc.* **1965**, *87*, 3787. [f] Onak, T.; Williams, R. E.; Weiss, H. G. *J. Am. Chem. Soc.* **1962**, *84*, 2830. [g] Spielman, J. R.; Warren, R. G.; Bergquist, D. A.; Allen, J. K.; Marynick, D.; Onak, T. *Synth. React. Inorg. Met.-Org. Chem.* **1975**, *5*, 347. [h] Olsen, R. R.; Grimes, R. N. *Inorg. Chem.* **1971**, *10*, 1103. [i] Reilly, T. J.; Burg, A. B. *Inorg. Chem.* **1973**, *12*, 1450. [j] Grimes, R. N. *J. Am. Chem. Soc.* **1966**, *88*, 1895. [k] Muetterties, E. L.; Balthis, J. H.; Chia, Y. T.; Knoth, W. H.; Miller, H. C. *Inorg. Chem.* **1964**, *3*, 444. [l] Pretzer, W. R.; Rudolph, R. W. *J. Am. Chem. Soc.* **1973**, *95*, 931. [m] Arafat, A.; Baer, J.; Huffman, J. C.; Todd, L. J. *Inorg. Chem.* **1986**, *25*, 3757. [n] Leyden, R. N.; Hawthorne, M. F. *J. Chem. Soc., Chem. Commun.* **1975**, 310. [o] Andersen, E. L.; Haller, K. J.; Fehlner, T. P. *J. Am. Chem. Soc.* **1979**, *101*, 4390. Haller, K. J.; Andersen, E. L.; Fehlner, T. P. *Inorg. Chem.* **1981**, *20*, 309. [p] Housecroft, C. E. *Inorg. Chem.* **1986**, *25*, 3108. [q] Vites, J.; Housecroft, C. E.; Eigenbrot, C.; Buhl, M. L.; Long, G. J.; Fehlner, T. P. *J. Am. Chem. Soc.* **1986**, *108*, 3304. [r] Wong, K. S.; Scheidt, W. R.; Fehlner, T. P. *J. Am. Chem. Soc.* **1982**, *108*, 1111. Housecroft, C. E.; Fehlner, T. P.; Buhl, M. L.; Long, G. J. *J. Am. Chem. Soc.* **1987**, *109*, 3323. [s] Khattar, R.; Puga, J.; Fehlner, T. P.; Rheingold, A. L. *J. Am. Chem. Soc.* **1989**, *111*, 1877. [t] Feilong, J.; Fehlner, T. P.; Rheingold, A. L. *Angew. Chem., Int. Ed. Engl.* **1988**, *27*, 424. [u] Feilong, J.; Fehlner, T. P.; Rheingold, A. L. *J. Am. Chem. Soc.* **1987**, *109*, 1860. [v] Meng, X.; Rath, N. P.; Fehlner, T. P. *J. Am. Chem. Soc.* **1989**, *111*, 3422.

a boron atom in a highly metallic environment. Furthermore, contrary to the earlier empirical results,[11] the chemical shifts of both metallaboranes containing $Fe(CO)_3$ and CoCp fragments are well reproduced by the calculations.

Calculations of ^{11}B chemical shifts for boranes have been reported earlier. For example, the INDO method has been used in a different theoretical approach (the finite perturbation theory) and yields an equal or slightly better fit to the observed shifts.[17] However, in order to obtain the INDO correlation, a reparametrization of the INDO method was required using a subset of the chemical shifts, and the newly optimized parameters were not the same as those used to fit other properties of the molecules. Thus, a big difference between this approach and the one reported here is that the MO's used by us are parameter free and identical with those used to describe other properties of the electronic structure.

After this manuscript was submitted, we learned of two additional pertinent studies, which have now appeared in part. First, the application of the IGLO method to the calculation of the chemical shifts of boranes and heteroboranes gives agreement with experiment an order of magnitude better than those reported here.[18] However, systems containing transition-metal atoms cannot be treated at the present time. Second, a mechanism for the antipodal effect (see below) has been postulated on the basis of an analysis of semiempirical Mulliken charges.[19]

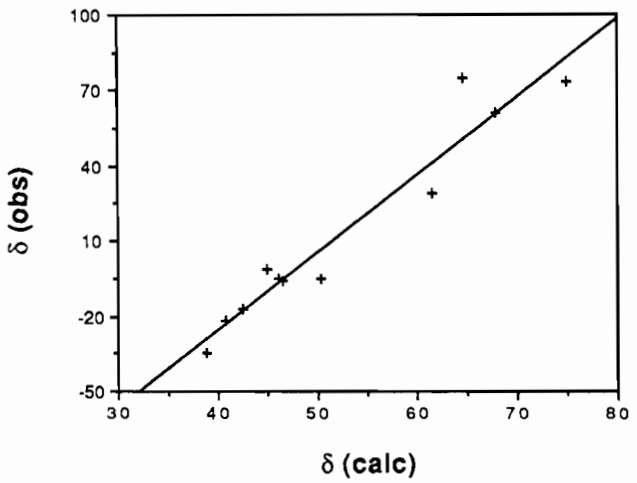

Figure 3. Correlation of δ(obs) and δ(calc) for all 10-atom closo cages in Table I. The equation of the straight line is $y = -149.2413 + 3.0881x$; $R = 0.97$.

(17) Ellis, P. D.; Chou, Y. C.; Dobh, P. A. *J. Magn. Reson.* **1980**, *39*, 529.
(18) Schleyer, P. R.; Bühl, M.; Fleischer, U.; Koch, W. *Inorg. Chem.* **1990**, *29*, 153.

Scheme II

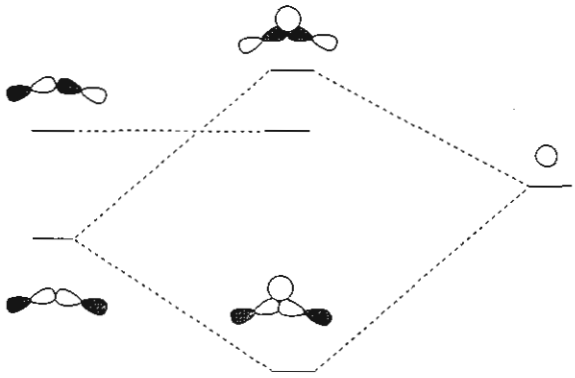

Table II. Change in the Components of σ_p in the Deprotonation of $HFe_4(CO)_{12}BH_2$

component[a]	$HFe_4(CO)_{12}BH_2$	$[Fe_4(CO)_{12}BH_2]^-$	difference
z	−41.38	−48.69	−7.31
x	−41.78	−49.48	−7.70
y	−31.50	−34.97	−3.47

[a] See Chart I for coordinate system.

Origin of Large Low-Field Shifts. Equation 2 not only reproduces the unusually large chemical shifts associated with metal-rich metallaboranes but also permits a physically reasonable explanation. Take, for example, the observed 34 ppm upfield shift in going from $[HFe_4(CO)_{12}BH]^-$ to $HFe_4(CO)_{12}BH_2$. The essence of the effect may be understood by reviewing the effect of protonating a bond formed from two B_{2p} functions. As shown in Scheme II, protonation results in a highly stabilized (3–4 eV from photoelectron spectroscopic studies[20]) filled bonding MO and highly destabilized unfilled antibonding MO. The former antibonding MO now becomes a nonbonding unfilled MO. The same argument holds for a bond formed from a B_{2p} AO and, for example, a Fe^{3d} AO. In $[HFe_4(CO)_{12}BH]^-$ the large B_{2p_y} AO component of the high-lying Fe–B bonding MO (or MO's) will make a contribution to only the L_z and L_x components of σ_p, e.g., for L_z only $\langle B_{2p_y}|L_z|B_{2p_x}\rangle$ and $\langle B_{2p_x}|L_z|B_{2p_y}\rangle$ are nonzero (see Chart I for the coordinate system). Protonating the Fe–B bond will result in a large reduction of this contribution to the overall shielding because of the large increase in ΔE. This reasoning is confirmed by the results shown in Table II. The change in the L_z and L_x components of σ_p on protonation constitutes 80% of the overall calculated change, and the energies and AO character of the specific filled MO's involved are of the type qualitatively depicted in Scheme II.

In general, it is known from calculations as well as photoelectron spectroscopic studies[21] that as one converts E–E (E = main-group atom) to E–M (M = transition-metal atom) to M–M interactions, the associated filled MO's rise in energy. In an analogous fashion to protonation, it follows that increasing the number of M–B direct interactions should introduce more B_{2p} character into high-lying filled MO's thereby leading to larger contributions to σ_p. This accounts in a qualitative fashion for the reported empirical relationship[12] between low-field chemical shift and number of M–B interactions; however, in any specific case, the MO picture requires detailed analysis such as that described above for $HFe_4(CO)_{12}BH_2$. In the following, we present another such detailed analysis for smaller, more symmetrical cages where mechanistic explanations involve fewer MO's of less complexity.

Exo-Substituent Effects. In a deltahedral main-group cage an exo-cage substituent causes a substantial upfield shift of the cross-cage boron atom while only slightly perturbing the other

Chart I

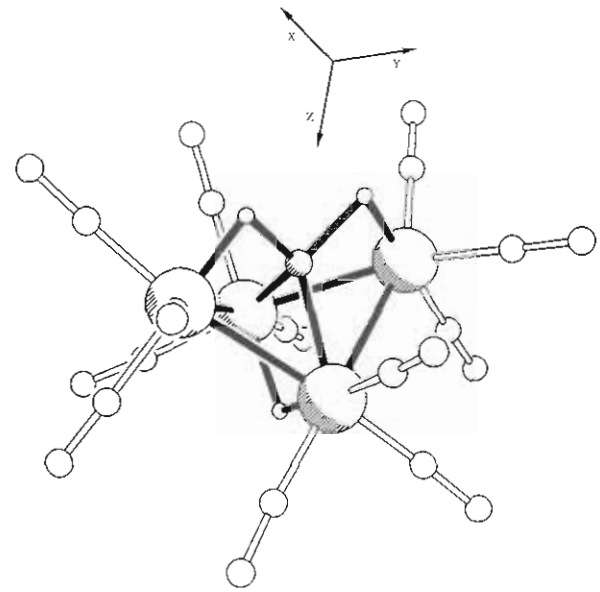

Chart II

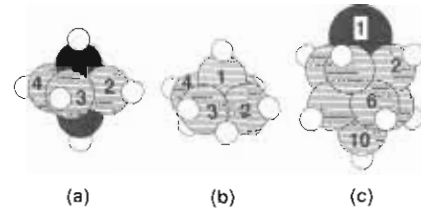

boron atoms that are not directly substituted. This substituent effect has been labeled the "antipodal effect" and has been the subject of a number of papers.[9,22] The attempts to provide an explanation of the effect are, thus far, basically empirical in nature, and hence, we have investigated the antipodal effect using the SOS approximation and Fenske–Hall molecular orbitals and energies. Our objective was to see if the observed shifts could be reproduced numerically and, if so, to construct a "mechanism" for the effect based on the MO's of the cage systems.

Two systems were explored: 2-X-1,6-$C_2B_4H_5$ and 2-XB_5H_8 where X = F, Cl, Br, I, and Me. The results are summarized in Table III, and the structures and numbering systems are defined in Chart IIa,b. The data are presented in two ways: the difference between the antipodal shift and that of the same boron atom in the unsubstituted parent and the difference between the trans boron atom (antipodal) and the cis boron atom. Clearly, the calculations yield the direction of the shifts in a satisfactory fashion even though the quantitative effects of individual substituents are more poorly reproduced. Despite this, the general trend in the magnitude of the substituent shifts are correctly given by the calculations. Thus, the changes in the occupied and unoccupied MO's and associated energies leading to the decrease of σ_p of the boron atom trans to the position of exo-cage substitution should provide an explanation of the antipodal substituent effect. To keep the problem tractable, we restrict our discussion to the 1,6-$C_2B_4H_6$ cluster and its exo-substituted chlorine derivative, 2-Cl-1,6-$C_2B_4H_5$. Presumably, the same explanation, albeit in a less simple form, applies to less symmetrical and/or larger cluster systems. The

(19) Hermanek, S.; Hnyk, D.; Havlas, Z. *J. Chem. Soc., Chem. Commun.* **1989**, 1859.
(20) Brundle, C. R.; Robin, M. B.; Basch, H.; Pinsky, M.; Bond, A. *J. Am. Chem. Soc.* **1970**, *92*, 3863.
(21) Vites, J.; Fehlner, T. P. *J. Electron Spectrosc. Relat. Phenom.* **1981**, *24*, 215.
(22) Tucker, P. M.; Onak, T. P. *J. Am. Chem. Soc.* **1969**, *91*, 6869. Tucker, P. M.; Onak, T.; Leach, J. B. *Inorg. Chem.* **1970**, *9*, 1430. Hermánek, S.; Gregor, V.; Stíbr, B.; Plesek, J.; Janousek, Z.; Antonovich, B. A. *Collect. Czech. Chem. Commun.* **1976**, *41*, 1492. Stanko, V. I.; Babushkina, T. A.; Klimova, T. P.; Goltiapin, Y. V.; Klimova, A. I.; Vasilev, A. M.; Alimov, A. M.; Khrapov, V. V. *Zh. Obshch. Khim.* **1976**, *46*, 1071. Siedle, A. R.; Bodner, G. M.; Garber, A. R.; Beer, D. C.; Todd, L. J. *Inorg. Chem.* **1974**, *10*, 2321. Hermánek, S.; Plesek, J.; Gregor, V.; Stíbr, B. *J. Chem. Soc., Chem. Commun.* **1977**, 561.

Table III. Calculated and Observed Substituent Shifts for 2-X-1,6-$C_2B_4H_5$ and 2-XB_5H_8

F		Cl		Br		I		Me	
Δδ(obs)	Δδ(calc)	Δδ(obs)	Δδ(calc)	Δδ(obs)	Δδ(calc)	Δδ(obs)	Δδ(calc)	Δδ(obs)	Δδ(calc)
				2-X-1,6-$C_2B_4H_5$[a]					
	−3.52	−9.3	−3.59	0.5	−2.46	−1.4	−1.88	−0.6	−0.67
	[−3.34]	[−11.6]	[−3.67]	[−1.9]	[−2.35]	[−4.2]	[−2.27]	[−4.2]	[−0.76]
				2-XB_5H_8[a]					
20.9	−2.01	−10.0	−1.92	−6.5	−1.30	−1.0	−0.93	−5.9	−0.43
[−16.0]	[−1.34]	[−9.7]	[−1.55]	[−6.0]	[−1.11]	[−3.0]	[−1.06]	[−5.4]	[−0.49]

[a] The first line of the table contains $\delta_{B(trans)} - \delta_{B(unsubst)}$ and the second line contains $\delta_{B(trans)} - \delta_{B(cis)}$ in brackets.

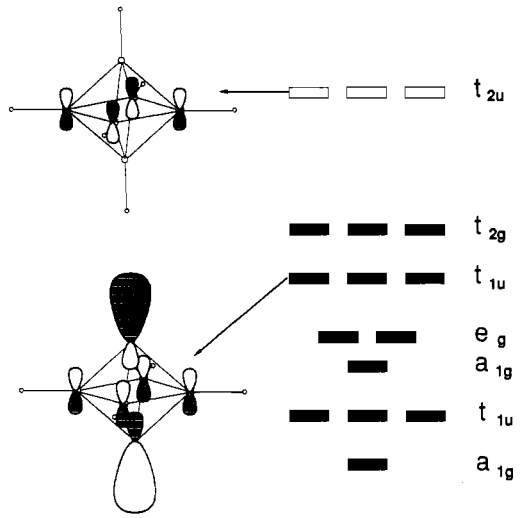

Figure 4. Schematic diagram of the MO structure of $[B_6H_6]^{2-}$. The filled boxes indicate populated MO's and representations of one component each of the t_{1u} and t_{2u} MO's important in explaining the antipodal effect are shown to the left.

problem is to sort out contributions to eq 2 for the unsubstituted cluster that change on substitution at the trans (antipodal) boron atom but not at the cis boron atom.

Figure 4 reviews the MO structure of $[B_6H_6]^{2-}$, which is the isoelectronic parent of 1,6-$C_2B_4H_6$[23] and illustrates two principal MO types that are shown below to be important in generating the antipodal effect. There are 13 filled MO's of which 6 (t_{1u}, e_g and a_{1g}) are assigned to exo-cluster bonding and 7 (t_{2g}, t_{1u} and a_{1g}) to endo-cluster bonding. Of the latter set, only the t_{2g} MO's are strictly endo-cluster bonding. For example, mixing between the t_{1u} sets leads to a higher lying t_{1u} set with (in the Fenske–Hall solutions) nearly equal contributions of endo- and exo-cage bonding character (Figure 4). Without such mixing, the critical t_{1u} set would lie at lower energy and the overall antipodal effect would be correspondingly reduced. The LUMO of t_{2u} symmetry is the antibonding partner of the t_{1u} endo-cage bonding MO.

Figures 5 and 6 schemically illustrate terms in eq 2 constituting the two major sources of the antipodal effect in a six-atom carborane cage. At the top of each figure is a diagram for the unsubstituted molecule showing MO numbers, ΔE, approximate B_{2p} AO contributions (size of lobes), and the overall contribution to σ_p. At the bottom of each is a diagram for the corresponding chloro-substituted molecule with the same information.

Figure 5 shows the largest contribution to the L_y term for σ_p in substituted and unsubstituted carborane cages. For both cases, the occupied MO is derived from the t_{1u} set of $[B_6H_6]^{2-}$ while the unoccupied MO comes from the t_{2u} set. In going from the parent carborane to the chloro derivative one must consider that additional MO's in the latter arise from the chlorine "lone pairs". The perturbation of these orbitals on the parent cluster yields molecular orbitals with similar symmetry to the original ones, but often very different AO coefficients. The destabilizing effect of the halogen is equivalent for both the occupied and unoccupied orbitals as

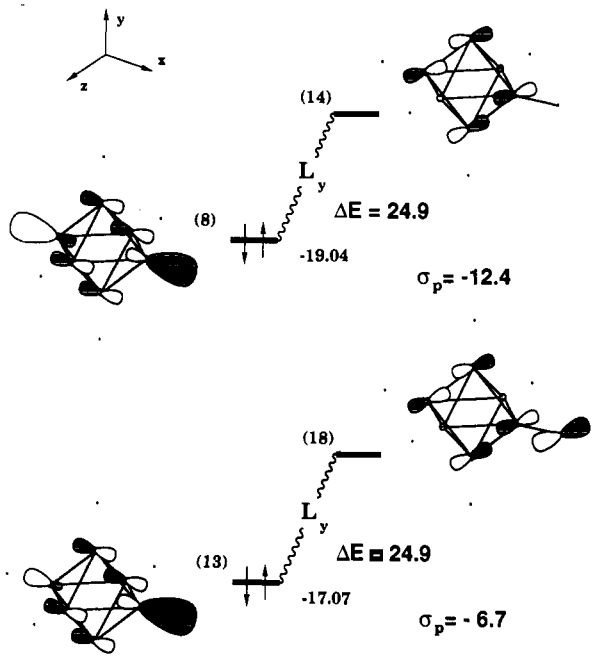

Figure 5. Schematic illustration of the contribution of the L_y term in eq 2 to σ_p for 2-X-1,6-$C_2B_4H_5$: X = H (top); X = Cl (bottom). The energies are in eV and the σ_p values are in ppm.

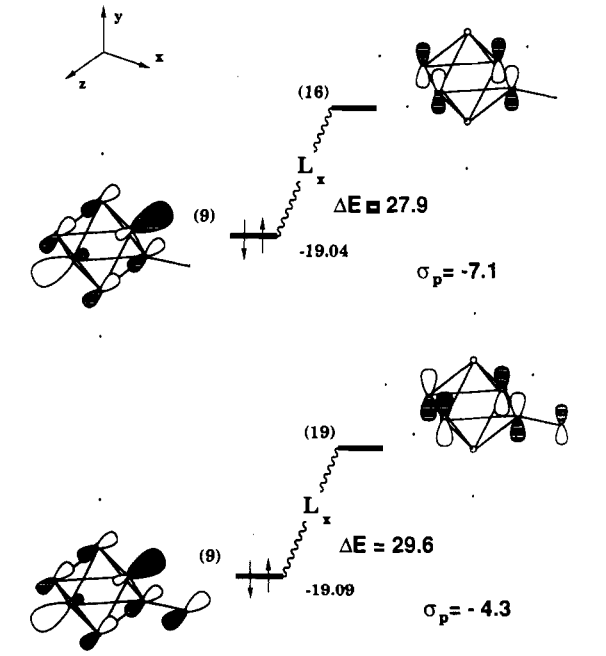

Figure 6. Schematic illustration of the contribution of the L_x term in eq 2 to σ_p for 2-X-1,6-$C_2B_4H_5$: X = H (top); X = Cl (bottom). The energies are in eV and the σ_p values are in ppm.

shown in Figure 5. As a result, the large decrease in σ_p upon substitution lies in the reduction of the B_{2p} AO coefficient at the antipodal boron in the occupied MO. The "polarization" of MO

(23) Hoffmann, R.; Lipscomb, W. N. *J. Chem. Phys.* **1962**, *36*, 2179.

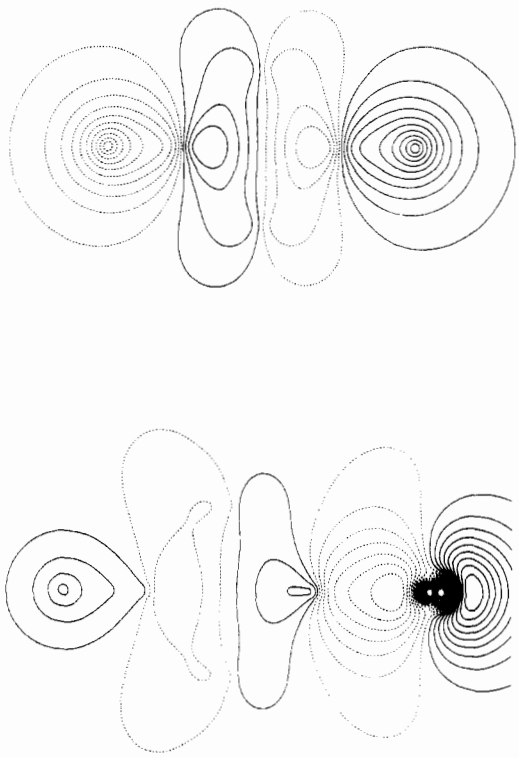

Figure 7. Contour plots of MO 8 (top) and MO 13 (bottom) in the B_4 plane for 1,6-$C_2B_4H_6$ and 2-Cl-1,6-$C_2B_4H_5$, respectively. Contour intervals are 0.03 au^{-3} with 20 contours plotted for MO 8 and 30 for MO 13.

13 is nicely illustrated by the MO contour diagrams shown in Figure 7 and directly results from a partitioning of the antipodal B_{2p} character between MO 13 and a lower lying orbital that is polarized opposite the site of substitution. That is, the higher lying MO contains largely chlorine character while the lower one contains mainly antipodal boron character. This lower lying MO contributes little to σ_p both because of a larger ΔE and a smaller $\langle\Phi_j|L_m|\Phi_k\rangle$ (the nonlocal term). The corresponding pair of MO's (9/17) for the cis position leads to the same net contribution to σ_p as in the unsubstituted carborane cage simply because there is no "polarization", and the B_{2p} AO coefficient for the cis boron remains high.

The largest contribution of the L_x component of σ_p to the antipodal effect in the six-atom cage also involves orbitals derived from the t_{1u} and t_{2u} MO's of $[B_6H_6]^{2-}$ but, obviously, disposed in a different fashion with respect to the position of substitution. Now, one finds that the B_{2p} AO coefficients are independent of substitution. Figure 6 shows that the destabilization of the unoccupied MO by an antibonding interaction with the Cl substituent is not matched in the occupied MO, resulting in a larger ΔE. In addition, by virtue of the different sign of the Cl_{3p} AO contribution in occupied and unoccupied MO's the nonlocal term is also reduced. For the cis boron, the filled MO is destabilized the same amount as the empty one, i.e., exactly as illustrated in Figure 5 for L_y.

Although there are other terms in eq 2 that contribute, the two illustrated in Figures 5 and 6 serve to delineate the basic orbital mechanism for this exo-cage substituent effect. The mixing of exo and endo characters results in high-lying hybrid filled MO's that contribute significantly to σ_p by "coupling" via the SOS approximation with unoccupied endo-cage MO's. On substitution, these MO's that intrinsically connect the position of substitution with its antipode are perturbed by "polarization" of the occupied MO's and destabilization of the unoccupied MO's by the halogen substituent.

One wonders if any corroborative evidence exists for such an explanation of the antipodal effect. This mechanistic picture suggests that the magnitude of the antipodal effect will be related to the strength of the interaction of the substituent with cage. The

Table IV. MO Origins of the Antipodal Effect in 10-Atom Closo Cages XB_9H_9

X	MO's[a]	L_α	σ_p(rel)	% B(occ)	% B(unocc)	E_{occ}, eV	E_{unocc}, eV
$[BN]^{2-}$	17/22, 23	x	−8.2	11	17	−16.1[b]	3.4[b]
	18/22, 23	x	−8.2	11	17	−16.1[b]	3.4[b]
	15/23	z	−6.4	10	17	−17.1[b]	3.4[b]
	15/22	y	−6.4	10	17	−17.1[b]	3.4[b]
NH	20/22, 23	x	−14.2	19	18	−15.0	−1.9
	21/22, 23	x	−14.2	19	18	−15.0	−1.9
	17/23	y	−14.2	29	18	−18.0	−1.9
	17/22	z	−14.2	29	18	−18.0	−1.9

[a] In the case of degenerate sets, only one pair is listed. [b] Corrected by −11.51 eV to match lowest energy totally symmetric cluster MO energy with that of the neutral molecule.

substituent interactions in 2-X-1,6-$C_2B_4H_5$, X = Cl, Br, and I, have previously been experimentally characterized by utilizing photoelectron spectroscopy.[24] The strength of the interaction of a substituent with the cage based on experimental splitting parameters decreases in the order Cl > Br > I. This matches the order of the calculated magnitudes of the antipodal effect (Table III). A similar experimental ordering is found for the halogenated pentaboranes.[25] Thus there is reason to believe that the Fenske–Hall–SOS approach can serve as a bridge between NMR observations and other spectroscopic data interpreted in a MO model.

Endo-Substituent Effects. Endo-cage substitution is defined as that in which an isolobal fragment replaces a BH fragment in a cage. In closo cages, this type of substitution also leads to characteristic shifts in the ^{11}B resonance of the antipodal boron atom. However, now the effects are much larger and the shifts are to lower rather than higher field. Apparently this antipodal effect was first observed in the SB_9H_9 10-atom closo cage (Chart IIc).[26] The B(10) boron resonance was found at δ 74.5, which is about 50 ppm to lower field than expected based on $[B_{10}H_{10}]^{2-}$. Similar antipodal shifts have been reported in several other 10-atom cages (Table I), but the observations were accompanied with little or no comment concerning the origin of the effect. Hence, it constitutes a good test of the Fenske–Hall–SOS approach particularly as the sign of the effect is opposite to that of exo-cage substitution. Note that the change in sign cannot be due to the larger cage size as there is evidence in the literature for an upfield antipodal exo-cluster substituent shift for chlorinated $[B_{10}H_{10}]^{2-}$.[27]

As shown in Table I and Figure 3, the calculations reproduce the endo-cage substituent effects very well both in terms of the direction of the antipodal shift as well as the shifts of the other cage boron atoms. Once again, σ_p alone appears sufficient to account for the observations and justifies exploring eq 2 for a mechanism for this substituent effect based on MO compositions and energies. To do so, we focus on $[B_{10}H_{10}]^{2-}$ and B_9H_9NH as a representative pair of cages.

Table IV lists the largest contributions to σ_p for the antipodal position (B(10)) in $[B_{10}H_{10}]^{2-}$ and B_9H_9NH in terms of occupied/unoccupied MO pairs, B_{2p} AO coefficients, and MO energies. A schematic representation of the pertinent MO's is given in Figure 8. Because of the different net charges on the compounds, the MO energies for the anion have been "normalized" to those of the neutral species by matching the energies of low-lying corelike MO's.[28]

Just as in the case of exo-cage substitution, there are two important types of interaction. If the principal symmetry axis is chosen to be the x axis, the largest contributions for the L_x operator involve the coupling of occupied and unoccupied MO's containing B_{2p} functions tangential to the cluster surface while those for the L_y and L_z operators contain radial and tangential B_{2p} character. When going from $[B_{10}H_{10}]^{2-}$ to B_9H_9NH the

(24) Beltram, G. A.; Fehlner, T. P. *J. Am. Chem. Soc.* **1979**, *101*, 6237.
(25) Ulman, J. A.; Fehlner, T. P. *J. Am. Chem. Soc.* **1976**, *98*, 1119.
(26) Rudolph, R. W.; Pretzer, W. R. *J. Am. Chem. Soc.* **1973**, *95*, 931.
(27) Curtis, Z. B.; Young, C.; Dickerson, R.; Lai, K. K.; Kaczmarczyk, A. *Inorg. Chem.* **1974**, *13*, 1760.
(28) Fenske, R. F.; De Kock, R. L. *Inorg. Chem.* **1972**, *11*, 437.

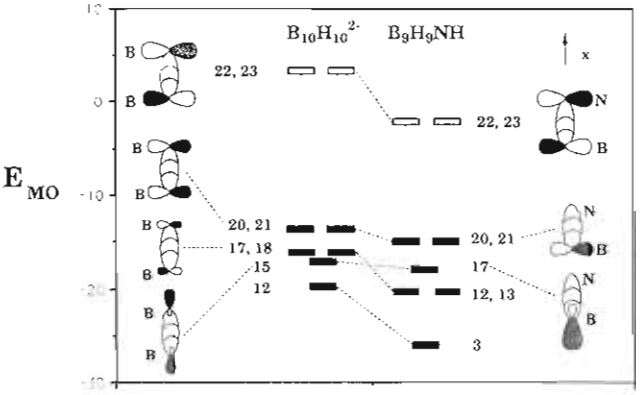

Figure 8. MO correlation diagram for XB_9H_9, X = $[BH]^{2-}$, and NH, for the MO's with large B_{2p} coefficients at the B(10) position. In the structural sketches, the NH fragment is at the top and the B(10) position is at the bottom of the cage schematic.

contributions to σ_p of both types roughly double in size. As shown in Table IV, the antipodal B_{2p} coefficients increase in the occupied MO's whereas there is a general reduction in ΔE values. Hence, in contrast to the smaller B_{2p} contributions and larger ΔE's produced by exo substituents, endo substitution produces changes in the opposite direction. The question is why?

The answer is evident in Figure 8. Let us consider the L_x contribution first. There are two parts to the explanation. The principal contributions from the L_x term for the antipodal boron in $[B_{10}H_{10}]^{2-}$ arise from the coupling of MO's 17 and 18 with MO's 22 and 23 even though MO's 20 and 21 have much larger B_{2p} coefficients and are closer in energy to the unfilled MO's! The reason for this is that the nonlocalized term in eq 2, $\langle\Phi_j|L_\alpha|\Phi_k\rangle$, is zero for the combinations MO 20, 21/MO 22, 23 by symmetry. That is, all nonzero couplings between molecular orbitals that contain antipodal p_y and p_z character will be negated by couplings of p_y and p_z orbitals on B(1) that are exactly the same in magnitude (same coefficients due to symmetry) but are opposite in sign. In going to the heterocluster, the symmetry is broken and MO's 20 and 21 (with the higher B_{2p} coefficient) now contribute. MO's 12 and 13, the analogue of MO's 17 and 18 of $[B_{10}H_{10}]^{2-}$, now contain some nitrogen character, fall to lower energy, and are less important. There is also a substantial ΔE effect that enhances the paramagnetic term in the heterocluster; a large reduction in the energy of the unoccupied MO pair occurs. It is well-known that when a fragment in a molecule is replaced by an isoelectronic but more electronegative fragment, both empty and filled MO's with significant heteroatom character are stabilized.

Consider the $L_{y,z}$ contribution next. First, the unoccupied MO's involved are exactly the same as for the L_x contribution. Second, notice that in $[B_{10}H_{10}]^{2-}$ MO's 12 and 15 contain the B_{2p_x} character equally divided between B(1) and B(10). Replacement of $[BH]^{2-}$ with NH leads to a splitting of the corresponding MO's (3 and 17). Again the higher MO contains more character of the electropositive boron atom, thereby leading to a larger σ_p.

Consequently, the endo-cage substituent effect can be ascribed to the existence of a set of cage MO's that contain an intrinsic connection between the antipodal positions. The pertinent unoccupied MO's undergo a large stabilization when a borane fragment is replaced by a more electronegative fragment while the pertinent occupied MO's undergo a partitioning of the antipodal B_{2p} character such that the higher energy MO contains a large percentage of the electropositive boron atom. Both changes lead to larger σ_p and downfield chemical shifts. We would then predict that a hetero fragment of similar electronegativity to that of the borane fragment would lead to a much smaller endo-cage antipodal effect. It is interesting to note that the recently characterized 12-atom closo cluster $[B_{11}H_{11}AlMe]^{2-}$ shows no exceptional downfield shift of the antipodal boron resonance.[29]

(29) Getman, T. D.; Shore, S. G. *Inorg. Chem.* **1988**, *27*, 3440.

Conclusions. This approach is far from "state of the art" as far as shielding calculations are concerned as it suffers from the neglect of the diamagnetic term. Still it provides a workable approach to an understanding of how some of the important features of MO structures of complex molecules give rise to chemical shift changes. The qualitatively important orbital interactions are correctly translated into relative shielding changes despite the approximate approach. In part, this is due to symmetry considerations and, thus, independent of the method. In making these connections, this approach has the potential of enhancing the usefulness of chemical shift data on complex molecules for the empirical chemist.

Acknowledgment. The support of the National Science Foundation is gratefully acknowledged. T.F. appreciates the hospitality of the chemistry department of the University of Wisconsin and the support provided by a Guggenheim fellowship.

Appendix. The molecular orbital calculations were completed on a VAX 8650 computer using the Fenske–Hall approximate MO method.[6] Interatomic distances and angles were idealized from X-ray crystallographic data when available, while typical values were used for cage derivatives for which such data are unavailable.[30] A minimal basis set was employed in these calculations. Clementi's free atom double-ζ Hartree–Fock–Slater type orbitals[31] were used for the second-row elements as well as Cl and I. Only the valence p functions on each atom were kept in the double-ζ form. Xα–SW calculations were performed on P, S, Fe, Co, Ni, Br, and Rh following the method of Herman and Skillman.[32] For these atoms, a basis set of orthogonalized STO's that maximize overlap with the Xα–SW eigenfunctions was created.[33] The STO functions of these atoms were of single-ζ form, except for the valence p orbitals on phosphorus and sulfur and the valence d orbitals on the transition metals, all of which were double-ζ form. The hydrogen 1s exponent was set at 1.16. The exponents for the transition-metal valence s and p orbitals were set at 2.0. These functions are less diffuse than atomic results but are found to describe bonding in organometallic complexes more accurately.[34]

The solution of the SOS expression for the paramagnetic term of the chemical shift, σ_p, requires the evaluation of matrix elements for the L and L/r^3 operators. Our approach utilizes the same Slater-type atomic orbital basis functions that are used in the Fenske–Hall MO calculations. For the evaluation of the σ_p of a particular boron atom in a molecule, the operators were centered on that atom. The computer programs for our study were adapted from those used by Freier et al. in a Xα–SW study of the ^{13}C NMR shifts of some small organic molecules.[35] As in that study, a mixed analytical–numerical integration is performed.[14,36] All integrals associated with the matrix elements for the L operator were calculated while, for the matrix elements of the L/r^3 operator, all integrals except three-center terms were evaluated. The operators employed are those obtained from the standard x, y, and z components of the angular momentum operators by multiplying by i (the square root of -1). Once the atomic orbital results are calculated, a simple transfer to a molecular orbital basis is performed by using the coefficients associated with the appropriate Fenske–Hall eigenvectors.

(30) See the references in Table I. Lipscomb, W. N. *Boron Hydrides*; Benjamin: New York, 1963. Muetterties, E. L., Ed. *Boron Hydride Chemistry*; Academic Press: New York, 1975.
(31) Clementi, E.; Ramondi, D. L. *J. Chem. Phys.* **1963**, *38*, 2686.
(32) Herman, F.; Skillman, S. *Atomic Structure Calculations*; Prentice Hall: Englewood Cliffs, NJ, 1963.
(33) Bursten, B. E.; Fenske, R. F. *J. Chem. Phys.* **1977**, *67*, 3138. Bursten, B. E.; Jensen, J. R.; Fenske, R. F. *J. Chem. Phys.* **1978**, *68*, 3320.
(34) Fenske, R. F.; Radtke, D. D. *Inorg. Chem.* **1968**, *7*, 479. Fenske, R. F. *Pure Appl. Chem.* **1988**, *60*, 1153.
(35) Freier, D. G.; Fenske, R. F.; Xiao-Zeng, You. *J. Chem. Phys.* **1983**, *7*, 3526. Fenske, R. F. *Organometallic Compounds, Synthesis, Structure and Theory*; Shapiro, B., Ed.; Texas A&M Press: College Station, TX, 1983; p 305. Freier, D. G., Ph.D. Thesis, University of Wisconsin—Madison, 1981.
(36) Pitzer, R. M.; Kern, C. W.; Lipscomb, W. N. *J. Chem. Phys.* **1962**, *37*, 267. Harriman, J. E. *Theoretical Foundations of Electron Spin Resonance*, Academic: New York, 1978.